

Our Number **8682639**

Their Number **8680567**

Status **Shipped/Expédié**

Printed Date **12 Sep 2016**

Request From **Toronto Robarts Library**

Bibliographic Details

Title **Petroleum Transactions, AIME**

ISBN/ISSN

Control Number

Publisher **Society of Petroleum Engineers**

Article Details

Volume/Issue **216**

Article Title **The Instability of Slow, Immiscible, Viscous Liquid-Liquid Displacements in Permeable Media**

Article Author **R.L. Chuoke, P. van Meurs, C. van der Poel**

Article Date **1959**

Pagination **188-194**

Action	Date	Item Notes
REQUEST-Indication	06 Sep 2016 11:07:41	AMICUS No. 15800699

Location	Action	Date	Public Notes
To Toronto Gerstein Science Info Centre	Shipped	08 Sep 2016 16:09:57	nl

Rota **Toronto Gerstein Science Info Centre**

Pickup Location **Toronto Gerstein Science Info Centre**

The Instability of Slow, Immiscible, Viscous Liquid-Liquid Displacements in Permeable Media

R. L. CHUOKE
P. van MEURS
JUNIOR MEMBER AIME
C. van der POEL

SHELL DEVELOPMENT CO.
HOUSTON, TEX.

KONINKLIJKE/SHELL-LABORATORIUM
AMSTERDAM, THE NETHERLANDS

ABSTRACT

When an initially planar interface between two immiscible liquids is displaced at constant rate, U , normal to the front, instability will occur for all rates greater than a critical rate, U_c , given by

$$\left(\frac{\mu_2}{k_2} - \frac{\mu_1}{k_1}\right)U_c + (\rho_2 - \rho_1)g \cos(zz') = 0,$$

provided the Fourier decomposition of the spatial perturbation or deformation of the moving displacement front contains modes with wavelengths, λ , greater than a critical wavelength, λ_c , given by

$$\lambda_c = 2\pi \left[\frac{\sigma^*}{\left(\frac{\mu_2}{k_2} - \frac{\mu_1}{k_1}\right)(U - U_c)} \right]^{1/2}.$$

In these expressions, ρ , μ and k , with the subscripts 1 and 2 distinguishing the two liquids under consideration, are density, viscosity and effective permeability coefficients respectively; g is the absolute value of the acceleration due to gravity; and $\cos(zz')$ is the direction cosine between the vertical cartesian coordinate z' (positive upward) and the z coordinate normal to the initially plane macroscopic interface taken positive in the direction from Liquid 1 to Liquid 2. U is the average volumetric velocity (injected volume of liquid per unit time per unit of total area normal to z) and is positive for Liquid 1 displacing Liquid 2, negative for the reverse displacement; and σ^* is an effective interfacial tension (for displacements between parallel plates, $\sigma^* = \sigma$, the ordinary bulk interfacial tension).

Further, there is a wavelength of maximum instability given by

$$\lambda_m = \sqrt{3}\lambda_c.$$

For natural perturbations, this wavelength will predominate and characterize the form of the instability as a quasi-sinusoidal deformation, i.e., viscous fingers of peak-to-peak separation, λ_m .

Comparison of experiment with theory reveals that these considerations are reasonably valid for displacements in both parallel plate channels and unconsolidated glass powder packs.

These results are of particular interest for interpretation of data from laboratory experiments with regard to field applications. It is quite possible for λ_c , although small relative to the largest lateral dimension of the reservoir, to exceed the greatest lateral extent of the laboratory sample or model. If it does, frontal displacement

occurs in the laboratory experiments, and oil recovery attained is higher than that from the field.

INTRODUCTION

The purposes of this paper are to present theoretical and experimental evidence for occurrence of macroscopic instabilities in displacement of one viscous fluid by another immiscible with it through a uniform porous medium and to compare available experimental data with some predictions of a theory of instability developed by the first author.

The instabilities are referred to as macroscopic in the sense that spatially quasi-sinusoidal, growing fingers of the displacing liquid are formed, the width and peak-to-peak separation (wavelength) of which is large relative to a characteristic length of the particular permeable medium such as grain size.

Visual models of two kinds have been used to obtain observations: displacement of oil by water-glycerine solutions through the flow channel formed by closely spaced parallel plates and displacement of oil by water with and without initial interstitial water through unconsolidated glass powder packs, employing the technique of matching indices of refraction.

In all cases we have observed macroscopic instabilities or fingers under conditions predicted by the theory to be favorable for their occurrence.

The phenomenon discussed here is not the production of streamers due to gross inhomogeneities such as permeability stratification of the porous medium.

It is our object to show, on the contrary, that a quantitative prediction of finger spacing is possible in a porous medium known to be macroscopically homogeneous and isotropic throughout.

The importance of the phenomenon in its influence on the configuration of oil and water with respect to oil production behavior was noted earlier by Engelberts and Klinkenberg¹ who coined the term "viscous fingering".

THEORY

NECESSARY AND SUFFICIENT CONDITIONS FOR INSTABILITY AND INITIAL KINEMATICS

There are several levels of increasing complexity in the theoretical description of instability of fluid displacements in permeable media. Of these, the simplest description, adapted to low permeability systems, is selected for presentation.² More inclusive descriptions are reserved for separate publication.

¹References given at end of paper.

Original manuscript received in Society of Petroleum Engineers office Aug. 1, 1958. Revised manuscript received March 23, 1959. Paper presented at 33rd Annual Fall Meeting of Society of Petroleum Engineers in Houston, Tex., Oct. 5-8, 1958.

First, consider the configuration of two liquids, labelled 1 and 2, each of infinite extent, with a plane, macroscopic interface moving slowly through a uniform permeable medium with speed, W , normal to the interface. This idealization is taken as a first working model for fluid displacements in both kinds of permeable media under consideration, although differences arise in interpretation.

An unperturbed immiscible displacement is characterized by a transition zone of steep saturation gradients of the displacing and displaced fluids. In the model, the transition zone is replaced by a sharp, plane, macroscopic interface to which are assigned pressure discontinuities preserving capillary properties of the transition zone and up to which are extrapolated the relatively uniform saturation and flow conditions prevailing outside the zone. The precise location of the macroscopic interface is not involved essentially in the following but may be determined by conservation of mass considerations. The model is directly amenable to the application of the most elementary form of first-order perturbation theory³ and finds partial justification within this framework through the assumption, implied in all of the following work, that only fundamental perturbation modes with wavelengths large relative to the width of the transition zone at the time of application of perturbation will be considered.

The assumption of uniform velocity implies, for constant rate displacements, equal initial and residual immobile saturations in the domains of the displaced and displacing fluids, respectively; however, this is not a fundamental restriction and it will be relaxed to allow non-equivalent saturations, provided these remain immobile.

Fluid displacement between closely spaced parallel plates is two-dimensional and involves only one microscopic fluid-fluid interface whereas displacements in a granular medium are three-dimensional, and the macroscopic interface represents many moving microscopic fluid-fluid interfaces. The formal mechanics of theory are the same and the results for parallel plate systems can be considered a specialization of those for granular systems; consequently, the following considerations apply to the latter systems.

A cartesian coordinate system is chosen with positive z axis directed from Fluid 1 to Fluid 2 perpendicular to the macroscopic interface and forming an angle (zz') with the z' axis of a fixed system of coordinates with positive z' directed vertically upwards. If Fluid 1 is displacing Fluid 2, W is a positive quantity. The z component of gravitational acceleration is $-g \cos(zz')$; thus, if the fluids are interchanged configurationally, the gravitational acceleration component as defined changes sign.

Macroscopic hydrodynamic equations of motion and continuity, a set for each fluid, are written as

$$\bar{v} = -\text{grad} \left\{ \frac{\kappa}{\mu} \left(p + \frac{\mu}{\kappa} Wz + \rho g [\cos(zz')]z \right) \right\} \quad (1)$$

$$= -\text{grad} \chi, \quad (2)$$

and

$$\text{div} \bar{v} = -\nabla^2 \chi = 0, \quad (3)$$

where $\bar{v} = (u, v, w)$ is a perturbation velocity. These equations are a description of fluid motion in a coordinate system moving with speed W in which the unperturbed interface is at rest. The origin of the x, y, z

system is presumed fixed in the plane of the unperturbed interface.

In writing Eq. 1 it is assumed that x and y components of gravitational force per unit volume of fluid are either negligible, as in the case of flow through closely spaced plates, or have been cancelled by respective pressure gradient components due to imposed tangential velocities. (In first-order theory, imposed tangential velocities have no effect on the form of results pertinent to instability. A second-order theory, however, predicts a form of Helmholtz instability.)

Eqs. 1 and 2 possess the integral,

$$p = \frac{\mu}{\kappa} \chi - \frac{\mu}{\kappa} Wz - \rho g [\cos(zz')]z + P(t), \quad (4)$$

where $P(t)$ is an arbitrary function of time.

If we decompose an arbitrary deformation of the macroscopic interface into fundamental Fourier perturbation modes and study each separately, the functional form of the deformation can be taken to be

$$\zeta = \varepsilon e^{n t + i(a_x x + a_y y)}, \quad (5)$$

where $i a_x + j a_y = \bar{\alpha}$ is the propagation vector in the x, y plane of magnitude

$$\alpha = (\alpha_x^2 + \alpha_y^2)^{1/2}, \text{ and } \varepsilon = \varepsilon(\alpha).$$

The kinematical conditions to be satisfied at the interface $z = \zeta$ are

$$\frac{\partial \zeta}{\partial t} = - \frac{\partial \chi_1}{\partial z} \Big|_{z=\zeta} = - \frac{\partial \chi_2}{\partial z} \Big|_{z=\zeta}, \quad (6)$$

with neglect of small quantities of the second order.†

The appropriate solutions of Eq. 3 are

$$\chi_1 = -n \alpha^{-1} \varepsilon e^{a_x x + i(a_y y) - a z}, \quad (7)$$

for Fluid 1, and

$$\chi_2 = +n \alpha^{-1} \varepsilon e^{-a z + n t + i(a_x x + a_y y)}, \quad (8)$$

for Fluid 2, for these make the z component of the perturbation velocity vanish at $z = \mp \infty$, respectively (constant rate displacement), and satisfy the kinematical conditions (Eq. 6) under the assumption that $\alpha \zeta$ is a small quantity (first-order theory).

At each point of the macroscopic interface there is conceived to be a pressure discontinuity consisting of two types of terms, i.e.,

$$(p_1 - p_2)_{z=\zeta} = \sigma^* (c_1 + c_2) + P_c(t), \quad (9)$$

where $P_c(t)$ is independent of curvature of the macroscopic interface but may be a function of time and is related to the capillary pressure drops across the microscopic fluid-fluid interfaces underlying the macroscopic interface; whereas σ^* is an effective interfacial tension and c_1, c_2 are the signed principal curvatures of the macroscopic interface, to be taken as negative when the respective center of curvature falls in the domain of Fluid 2.

The assumption that $\alpha \zeta$ is small allows the approximations,

† Let $F(x, y, z, t) = 0$ be the equation of the interface. At every point of this surface,

$$\frac{DF}{Dt} = \frac{\partial F}{\partial t} + u \frac{\partial F}{\partial x} + v \frac{\partial F}{\partial y} + w \frac{\partial F}{\partial z} = 0.$$

Since $F = z - \zeta$,

$$\frac{\partial \zeta}{\partial t} + u \frac{\partial \zeta}{\partial x} + v \frac{\partial \zeta}{\partial y} = w.$$

and Eq. 6 follows from the definitions of the velocity potentials, χ_1 and χ_2 , and neglect of the terms

$$u \frac{\partial \zeta}{\partial x}, v \frac{\partial \zeta}{\partial y}.$$

$$c_1 \sim -\frac{\partial^2 \zeta}{\partial x^2}, \quad c_2 \sim -\frac{\partial^2 \zeta}{\partial y^2}.$$

Combining Eq. 4 with Eq. 9 results in

$$\frac{\mu_2}{\kappa_2} (\chi_2)_{z=z'} - \frac{\mu_1}{\kappa_1} (\chi_1)_{z=z'} - \left[\left(\frac{\mu_2}{\kappa_2} - \frac{\mu_1}{\kappa_1} \right) W + (\rho_2 - \rho_1) g \cos(zz') \right] \zeta - \sigma^* \left(\frac{\partial^2 \zeta}{\partial x^2} + \frac{\partial^2 \zeta}{\partial y^2} \right) + P_2(t) - P_1(t) + P_c(t) = 0.$$

According to Eqs. 5, 7 and 8, and for small $\alpha \zeta$, Eq. 10 leads to

$$P_1(t) - P_2(t) = P_c(t), \quad \dots \quad (11)$$

and to the characteristic equation,

$$\left(\frac{\mu_2}{\kappa_2} + \frac{\mu_1}{\kappa_1} \right) n - \left[\left(\frac{\mu_2}{\kappa_2} - \frac{\mu_1}{\kappa_1} \right) W + (\rho_2 - \rho_1) g \cos(zz') \right] \alpha + \sigma^* \alpha^3 = 0, \quad \dots \quad (12)$$

which determines n as a function of α and yields directly the kinematics of early growth.

Clearly, for $\alpha > 0$, the necessary and sufficient condition for instability, i.e., for n to be positive, is given by

$$\left(\frac{\mu_2}{\kappa_2} - \frac{\mu_1}{\kappa_1} \right) W + (\rho_2 - \rho_1) g \cos(zz') - \sigma^* \alpha^2 > 0 \quad \dots \quad (13)$$

Alternatively, introducing the effective permeabilities, k_1 and k_2 , and volumetric velocity, U , one may say that instability will occur for all velocities $U > U_c$ where U_c is a critical volumetric velocity defined by†

$$\left(\frac{\mu_2}{k_2} - \frac{\mu_1}{k_1} \right) U_c + (\rho_2 - \rho_1) g \cos(zz') = 0, \quad \dots \quad (14)$$

provided the perturbation contains wavelengths†† $\lambda = 2\pi/\alpha$ greater than a critical wavelength, λ_c , defined by

$$\lambda_c = 2\pi \left[\frac{\sigma^*}{\left(\frac{\mu_2}{k_2} - \frac{\mu_1}{k_1} \right) (U - U_c)} \right]^{1/2} \quad \dots \quad (15)$$

The inequality, $U > U_c$, is a necessary condition for instability, whereas $U > U_c$ and $\lambda > \lambda_c$ combined form the necessary and sufficient condition for instability equivalent to Eq. 13.

For $U > U_c$, the index of instability, n , as a function of α possesses an absolute maximum. The root,

$\alpha = \alpha_m$ of the equation, $\frac{\partial n}{\partial \alpha} = 0$, determines the wave-

length†† of maximum instability which is given in terms of the critical wavelength, λ_c , by

$$\lambda_m = \sqrt{3} \lambda_c \quad \dots \quad (16)$$

For two-dimensional systems or for $\alpha_x = \alpha_y$, there is a unique perturbation mode of greatest instability index which will grow exponentially in time during the early stages at the fastest rate relative to other funda-

mental perturbation modes present. Consequently, for natural or random perturbations, this mode will tend to predominate and reveal the instability of the system as a quasi-sinusoidal deformation of fluid configurations with peak-to-peak separation determined by λ_m .

For different immobile saturations of fluids in the two domains, which is equivalent to different initial velocities (W_1 and W_2) for constant injection rate, the representation of perturbative velocities as in Eq. 1 effectively represents the perturbative velocities in a coordinate system in which there is no initial motion of the fluids. Consequently, by the conditions of Eq. 6, which achieve continuity of the normal components of perturbative velocities and their equality with the interfacial velocity of the applied perturbation mode, the necessary and sufficient condition for instability is

$$\left(\frac{\mu_2}{\kappa_2} W_2 - \frac{\mu_1}{\kappa_1} W_1 \right) + (\rho_2 - \rho_1) g \cos(zz') - \sigma^* \alpha^2 > 0, \quad \dots \quad (17)$$

which again yields the conditions for instability, $U > U_c$ and $\lambda > \lambda_c$ (see Eqs. 14 and 15) when the effective permeabilities, k_1 and k_2 , and the constant injection rate, U , are used.

PRESSURE DISCONTINUITIES AT MACROSCOPIC INTERFACE; EFFECTIVE INTERFACIAL TENSION

That part of the pressure discontinuity labelled P_c in Eq. 9 is the pressure drop across the macroscopic interface of the model that preserves the rate of working by or against capillary forces in the unperturbed state; hence it may be a positive or negative magnitude.

In the process of deforming the macroscopic interface in such a way that $c_1 + c_2 \neq 0$, an additional rate of working against interfacial forces is required that is dependent upon the net rate of creation of microscopic fluid-fluid interfaces.

Let A^* represent the total area of the microscopic, moving fluid-fluid interfaces, and A the total area of the macroscopic interface. To the first order in the perturbative velocity, the total additional rate of working at each point of the macroscopic interface is given by

$$(p_1 - p_2)_{z=z'} \frac{\partial \zeta}{\partial t} dA = \sigma \frac{\delta(dA^*)}{\delta t} + P_c \frac{\partial \zeta}{\partial t} dA, \quad \dots \quad (18)$$

where σ is the ordinary bulk fluid interfacial tension and dA^* the element of total interfacial area associated with dA

By definition,

$$(p_1 - p_2)_{z=z'} \frac{\partial \zeta}{\partial t} dA = \sigma^* \frac{\delta(dA)}{\delta t} + P_c \frac{\partial \zeta}{\partial t} dA, \quad \dots \quad (19)$$

where σ^* is the effective interfacial tension.

Consequently,

$$\sigma^* = \sigma \left(\frac{\delta(dA^*)}{\delta t} / \frac{\delta(dA)}{\delta t} \right), \quad \dots \quad (20)$$

which implies, owing to the fact that A^* can be much greater than A , that σ^* may be considerably larger than σ .

In view of the fact that

$$\frac{\delta(dA)}{\delta t} = (c_1 + c_2) \frac{\partial \zeta}{\partial t} dA, \quad \dots \quad (21)$$

†Apparently, various forms of the inequality, $U > U_c$, have now been derived independently by several authors. To our knowledge, the inequality specialized to vertical flow was first derived in connection with instability problems of the type considered here by Hill⁴. See also Dietz⁵, and van der Poel and Killian⁶.

††In using the term wavelength in this context it must be remembered that since $\alpha = (\alpha_x^2 + \alpha_y^2)^{1/2}$, λ and λ_c do not directly give spacings of maxima or minima in the x, y plane except for α_x or α_y equal to zero, i.e., for two-dimensional perturbations. For

three-dimensional perturbations, if $\alpha_x = S\alpha_y$, i.e., $\lambda_y = \frac{2\pi S}{\alpha_y} = \frac{2\pi S}{\alpha_x}$,

then λ and λ_c in the statement pertaining to Eq. 15 may be taken as true wavelengths referring to spacings along the x or y axis provided the right-hand side of Eq. 15 is multiplied by $[(1 + S^2)/S^2]^{1/2}$ or $(1 + S^2)^{1/2}$, respectively.

Eq. 19 becomes

$$(p_1 - p_2)_{z=0} = \sigma^* (c_1 + c_2) + P_c, \quad (22)$$

which is Eq. 9 used in the preceding derivation.

For a parallel-plate system, this condition reduces to

$$(p_1 - p_2)_{z=0} = \sigma(c_1 + c_2) = \sigma c_1 + P_c, \quad (23)$$

since the perturbation curvature, c_1 , occurs only in the plane of flow determined by the plates and the original capillary pressure, $P_c = \sigma c_2$, due to the initial curvature of the single microscopic interface involved remains unperturbed. Consequently, the necessary and sufficient condition Eq. 13 or Eqs. 14 and 15 together are directly applicable to displacements in parallel-plate channels upon replacing σ^* by the bulk fluid interfacial tension σ .

EXPERIMENTAL

EXPERIMENTS WITH THE PARALLEL-PLATE MODEL

Two glass plates were spaced 1-mm apart to provide a uniform flow channel for displacing oil with water-glycerine solutions. The model was the same as that used in the study of production of attic oil described earlier⁶.

To obtain good reproducibility, the inner walls were made preferentially oil-wet with the help of silicones, and the oil was introduced first, i.e., the displacing fluid was non-wetting. In the experiments yet to be discussed the flow channel was tilted about 45° from the horizontal, and the water-glycerine mixture, rendered visible by addition of methylene blue dye, was injected at the lower end. After injection of a small amount of the glycerine mixture, injection was stopped and the fluids allowed to equilibrate under the action of gravity. At low rates of injection the moving interface remained essentially stable and no fingers were formed. As reported before⁶ it was found that fingering actually does not occur at rates below the critical rate given by Eq. 14.

We shall discuss here a set of three displacement experiments performed at rates above this critical rate. In these experiments density and viscosity of the oil and glycerine-water mixtures were constant with $\rho_2 = 0.877$ gm/cm³ and $\mu_2 = 1.39$ poise for oil and $\rho_1 = 1.21$ gm/cm³ and $\mu_1 = 0.552$ poise for glycerine-water. The system was tilted at an angle of 44°25'; the bulk interfacial tension between the fluids was 33 dyne/cm. Since

for the parallel-plate model, $\kappa = \frac{1}{12} h^2$, h being the

plate spacing equal to 1 mm, $\kappa = 1/1,200$ cm². Eq. 14 yields for the critical rate, $U_c = 0.23$ cm/sec.

Fig. 1 gives a time sequence (a,b,c,d) of photographs of experiments carried out at an injection rate about twice the critical value ($U = 0.41$ cm/sec). The instability of the moving interface resulting in the production of fingers is apparent from these photographs. The shape of these fingers is clearly seen, and it will be noticed that there is a dissimilarity between the form of the water fingers and that of the oil fingers.

Fingers of the less viscous liquid, here the water-glycerine solution, are the broader ones. Note also the characteristic bulbous tips of the fingers. These effects are thought to be partly due to difference in viscosity. The more viscous oil yields more slowly to the shearing stresses produced in forcing the oil ahead. This flattens the tips of the water fingers. Similar effects have been noticed by Avsec⁷ and may also be seen in the work of Lewis⁸. Nevertheless, the quasi-sinusoidal character of the deformation of the originally

straight interface is obvious from the pictures.

With increase in flow rate the number of fingers increased, as is seen from Fig. 2, which shows three photographs of experiments carried out with different injection rates at corresponding displacements of the flood "front" (Fig. 2a is identical with Fig. 1c). This is in agreement with Eqs. 15 and 16, which predict the smaller wavelengths of maximum instability for higher flow rates.

Since in the parallel-plate model σ equals σ^* , the wavelengths of maximum instability can be directly cal-

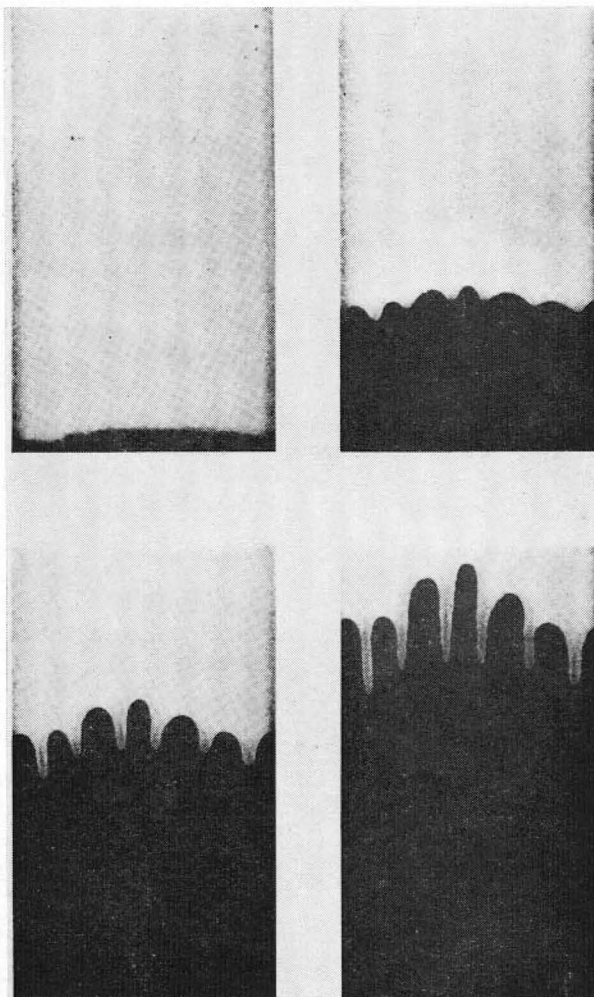


FIG. 1—INSTABILITY OF A WATER-OIL INTERFACE MOVING WITH UNIFORM NORMAL SPEED OF 0.41 CM/SEC AS COMPARED TO CRITICAL SPEED OF 0.23 CM/SEC IN A TILTED CHANNEL FORMED BY PARALLEL PLATES. ANGLE OF TILT, 45°; $\mu_1 = 0.552$ POISE; AND $\mu_2 = 1.39$ POISE.

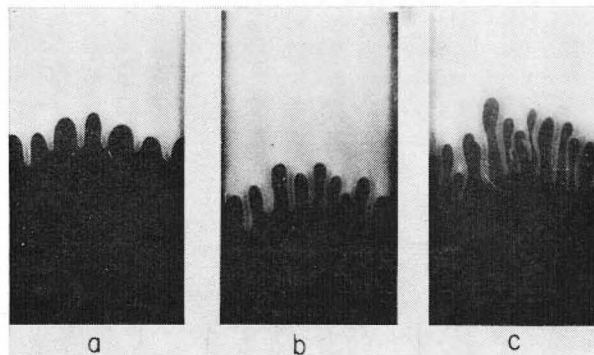


FIG. 2—THE EFFECT OF RATE ON FINGER SPACING AS OBSERVED IN TILTED CHANNEL FORMED BY PARALLEL PLATES. FLUIDS AND ANGLE OF TILT ARE SAME AS IN FIG. 1. (a) $U = 0.41$ CM/SEC, (b) $U = 0.87$ CM/SEC, AND (c) $U = 1.66$ CM/SEC.

TABLE 1—COMPARISON OF CALCULATED AND OBSERVED FINGER SPACING IN PARALLEL-PLATE MODEL

Fig. No.	U_0 (cm/sec)	$U_{exp.}$ (cm/sec)	Calc. λ_m (cm)	Obs. $\lambda_{avg.}$ (cm)
1 and 2a	0.23	0.41	4.6	3.5
2b	0.23	0.87	2.6	2.4
2c	0.23	1.66	1.6	1.7

culated. In accordance with interpretation of the theory given before, we compare this calculated λ_m with the average fingerspacing, $\lambda_{avg.}$, determined experimentally. Numerical results are given in Table 1.

The comparison between the observed and calculated wavelengths of maximum instability in this table is favorable to the interpretation as it stands; however, the centimeter difference in wavelength for the experiment illustrated in Fig. 1, an excellent illustration of fingers, may be associated with the observation that discrepancies are most likely to occur at the lower injection rates since, although the instability index, n , as a fraction of wavelength possesses a maximum for all rates, the maximum is the flatter, the lower the rate. It is therefore less probable that the wavelength of maximum instability will distinguish itself in the time span of exponential growth.

Fig. 3 illustrates this, for it is a plot of n as a function of λ as calculated from Eq. 12 for the three experiments under consideration. As is clear from this figure, the maximum for the lower rate experiment is not pronounced; this may explain the discrepancy observed.

EXPERIMENTS WITH TRANSPARENT POWDER PACK MODELS COMPLETELY SATURATED WITH OIL

With the transparent model technique reported earlier⁹, interesting results have been obtained pertaining to an actual porous medium. Two models were used, of dimensions 5 x 30 x 60 cm and 2 x 9 x 18 cm. The models were packed with Pyrex glass powder and completely saturated with oils having a refractive index identical to that of the Pyrex glass to render the glass pack transparent. At both ends of the models small chambers were provided separated from the glass pack by a wire screen. The chamber at the injection end was flooded out by the injection water before the experiment was started to ensure a planar interface at the start of the experiment. Since the injection fluid (water) has a refractive index differing from that of the glass grains and the oil, light is scattered wherever water has penetrated; these places show up white in the photographs.

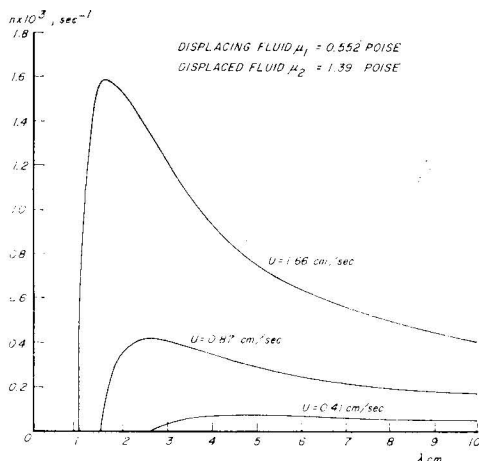


FIG. 3—PLOT OF INSTABILITY INDEX, n , AS A FUNCTION OF WAVELENGTH, λ , FOR THREE PARALLEL PLATE EXPERIMENTS.

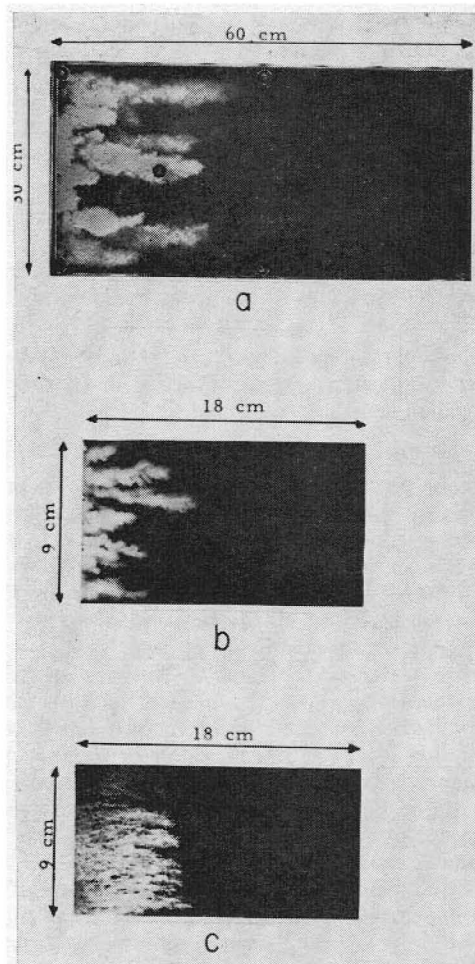


FIG. 4—THREE EXAMPLES SHOWING THE EFFECT OF OIL VISCOSITY AND BULK INTERFACIAL TENSION ON FINGER SPACING. DISPLACING WATER APPEARS WHITE. (a) $\mu_o = 9.45$ CP, $k = 96 D$, $\mu_w = 1$ CP, $U = 0.00932$ CM/SEC, AND $\sigma = 42$ DYNE/CM; (b) $\mu_o = 66$ CP, $k = 65 D$, $\mu_w = 0.936$ CP, $U = 0.0106$ CM/SEC, AND $\sigma = 48$ DYNE/CM; (c) $\mu_o = 202$ CP, $k = 65 D$, $\mu_w = c$ CP, $U = 0.00525$ CM/SEC, AND $\sigma = 3.5$ DYNE/CM.

The glass powder used in these experiments was carefully cleaned with acids and solvents. Its wettability condition can best be described as neutral. Photographs of three representative experiments are reproduced in Fig. 4.

In contrast to instabilities observed in the parallel plate model, the sides of the fingers in these pictures are not smooth but clearly show irregularities. Though not of special interest in the problem under discussion it does have a bearing on production behavior as shown in a recent paper¹⁰.

Comparison of Fig. 4a with Fig. 4b shows that when the oil viscosity is higher, smaller fingers are formed. Also the lower the bulk interfacial tension, the smaller the fingers as is demonstrated by comparison of Fig. 4b with Fig. 4c. These trends are in accordance with those predicted by the theory.

Since the value of σ^* in Eq. 20 is essentially unknown, no a priori numerical prediction of the wavelength of maximum instability can be given. It can, however, be shown that trends predicted by the theory are in numerical agreement with experimental data.

For systems of approximately neutral wettability, it is reasonable to assume that σ^* is directly proportional to σ . On this basis, for horizontal displacements such

that $U_o = 0$, and $k_1 = k_2 = k$, Eq. 16 in conjunction with Eq. 15 can be written as

$$\lambda_m = C \sqrt{\frac{\sigma k}{U(\mu_o - \mu_w)}}, \dots \dots \dots (24)$$

where C is a dimensionless constant of the order, $2\pi\sqrt{3}$.

The experimental data are found to fit this formula to a reasonable degree when the constant C is taken equal to 30. Characteristics of the experiments as well as the finger spacings measured are presented in Table 2.

Since all parameters have been varied in these experiments, agreement between theory and experiment may be called satisfactory.

FINGERING IN SYSTEMS CONTAINING CONNATE WATER

The same visual model technique has also been used to produce oil-saturated packs containing connate water. An aqueous solution of ammonium iodide of matching refractive index was first injected into a pack consisting of pyrex powder baked for several hours at 500°C. Upon displacement by oil of the same refractive index a transparent system containing up to 0.15 pore volume of connate water was obtained. This system imbibes water spontaneously and can be described as strongly water-wet. When pure water is injected into a model prepared this way, the phenomenon of various fingering is again clearly observed as is illustrated by the photograph of Fig. 5. Though quantitative data are still insufficient to test the theory thoroughly, it is clear that for such systems the constant, C , in Eq. 24 is larger than for the "neutral" systems discussed before. This is in accordance with the a priori expectation that σ^* should be larger for media which spontaneously imbibe water than for those which do not.

This also signifies that the critical wavelength, λ_c , for such water-wet systems is large and can easily exceed twice the lateral extent of the model or the core specimen. Under such conditions all observable wavelengths fall in the range of stability or decaying amplitudes; this may explain why, under laboratory conditions, the phenomenon of viscous fingering may not reveal itself even though the system satisfies the necessary condition for instability. In this connection, both a high viscosity difference and a high injection rate have been used for the Fig. 5 experiment.

APPLICATIONS

These results are of particular interest for interpretation of data from laboratory experiments with respect to field applications.

Even if the usual similarity groups¹ such as

$$\frac{\sigma\sqrt{k}}{U\mu_w d}, \frac{(\rho_o - \rho_w)g\sqrt{kd}}{\sigma}, \frac{\mu_o}{\mu_w}, \frac{l}{d}, \text{ etc.}$$

TABLE 2—COMPARISON OF CALCULATED AND MEASURED FINGER SPACING IN TRANSPARENT GLASS PACK

Fig.	σ No. (dyne/cm)	$k \times 10^8$ (cm ²)	U (cm/sec)	μ_o (poise)	μ_w (poise)	Calc.	Obs.
						$\lambda_m = 30 \sqrt{\frac{\sigma k}{U(\mu_o - \mu_w)}}$ (cm)	λ_{avg} (cm)
4c	3.5	64	0.00525	2.02	0.030	0.432	0.65
	4	64	0.0148	0.60	0.00914	0.51	0.67
	15	11.1	0.0020	0.66	0.00914	1.07	0.88
4b	48	64	0.0106	0.66	0.00936	1.97	1.45
	11	64	0.011	0.086	0.0090	2.72	2.1
	47	80	0.00133	1.86	0.0093	3.72	4.0
4a	42	94	0.00952	0.0945	0.0010	6.7	5.0
	47	80	0.0010	1.86	0.0093	4.3	5.5

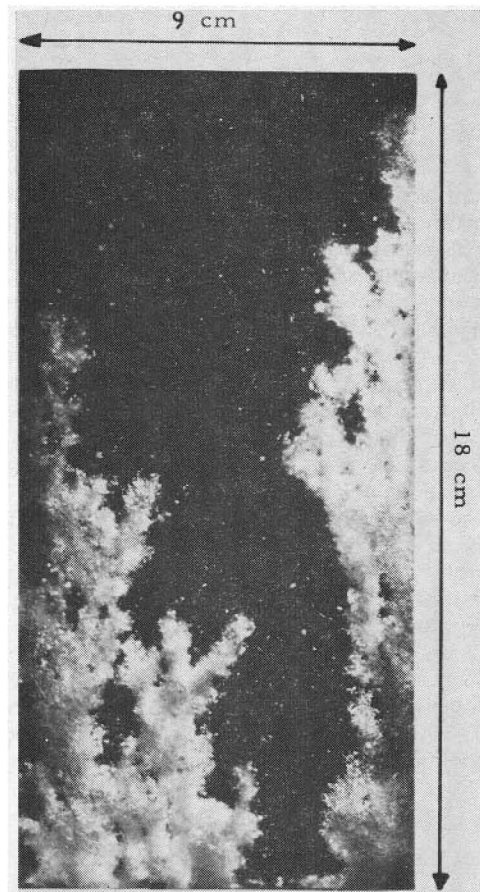


FIG. 5—FINGER FORMATION IN A POROUS OIL-BEARING MEDIUM CONTAINING 0.15 PORE VOLUMES OF CONNATE WATER. DISPLACING WATER APPEARS WHITE. $\mu_o = 200$ CP, $\mu_w = 1$ CP, $\sigma = 25$ DYNE/CM, $k = 200$ D, AND $U = 0.115$ CM/SEC.

are used to determine a model displacement experiment, results can be misleading if the phenomenon of viscous fingering occurs in the prototype, whereas in the laboratory experiment λ_c exceeds the greatest lateral dimension, d , of the model. In that case frontal displacement occurs in the model, leading to higher recoveries than in the reservoir.

Therefore, for unstable systems a properly scaled experiment also requires the dimensionless group,

$$\left(\frac{\lambda_m}{d}\right)^2 \text{ OR } \frac{\sigma}{\left[\left(\frac{\mu_o}{k_o} - \frac{\mu_w}{k_w}\right)(U - U_c)\right] d^2},$$

to be identical in model and prototype. To satisfy these conditions simultaneously, although not impossible in principle, is hardly feasible in practice.

There exist, however, possibilities of departure from strict adherence to the scaling rule pertaining to finger spacing, depending upon the range of λ_m/d in the reservoir.

We consider the three following cases.

1. $\lambda_m/d \ll 1$ in the prototype. This signifies a large number of fingers. It is our experience that as long as there are a sufficient number of fingers in the model (of the order of six or more), production behavior is insensitive to variations in the value of λ_m/d .

2. $\lambda_m/d \gg 1$ in the reservoir. Then the system has essentially a stable behavior, i.e., no fingers will occur; also in the model an essentially stable situation must be present, i.e., λ_m/d should be greater than one.

3. In the prototype λ_m is of the order of d . Production behavior can be seriously affected by the variations in the value of λ_m/d . Therefore in this case the value of this similarity group should be exactly the same in model and prototype.

Since for relative permeability measurements small cores are usually used, it is not improbable that in such a measurement λ_c exceeds twice the diameter of the sample. In such a core a saturation distribution exists which is certainly not representative for the fluid distribution in a cross section of an actual reservoir under conditions where viscous fingers are present.

NOMENCLATURE

- c_1, c_2 = signed principal curvatures of macroscopic interface
 d = greatest lateral extent of reservoir or model
 g = absolute magnitude of gravitational acceleration
 k = absolute permeability
 k_1 = effective permeability to fluid 1
 k_2 = effective permeability to fluid 2
 l = length of reservoir or model
 n = instability index, sec.⁻¹
 p = pressure
 P_c = effective capillary pressure
 S = saturation
 U = volumetric or superficial velocity, cm³ of fluid injected/cm² of total cross section x sec.
 v = perturbation velocity, cm³ of fluid/cm² of fluid cross section x sec.
 $W = U/\phi S$ = initial speed normal to the interface, positive when Fluid 1 displaces Fluid 2, negative otherwise, cm³ of fluid/cm² of fluid cross section x sec.
 z = cartesian coordinate normal to macroscopic interface, positive when directed from Fluid 1 to Fluid 2
 z' = cartesian coordinate, positive vertically upwards
 (zz') = angle between z and z' axes.

GREEK

- $\alpha = 2\pi/\lambda$ = wave number, cm⁻¹
 ε = initial amplitude of fundamental Fourier perturbation mode, cm

- ξ = fundamental Fourier perturbation, cm
 $\kappa_{1,2} = k_{1,2}/\phi S_{1,2}$
 λ = wavelength of fundamental perturbation, cm
 μ = absolute viscosity
 ρ = density
 σ = bulk interfacial tension
 σ^* = effective interfacial tension
 ϕ = porosity
 χ = velocity potential

ACKNOWLEDGMENTS

We wish to thank J. W. Killian and P. J. Closmann for stimulating discussions.

We are also indebted to Mr. H. Hooykaas for the experiment described in Section III C. and to L. W. Pickle and R. N. Hale for their assistance in carrying out the parallel-plate experiments.

REFERENCES

- Engelberts, W. F. and Klinkenberg, L. J.: "Laboratory Experiments on the Displacement of Oil by Water from Packs of Granular Materials", *Proc. 3rd World Petr. Congr., The Hague (1951) Part II*, 544.
- Theory and application to parallel-plate systems were presented at the Feb., 1956, Houston meeting of the American Physical Society. Abstract R5 by Robert L. Chuoke, *Bull. Am. Phys. Soc. Series II (1956) 1*, 98. Misprint corrected in *Erratum, Ibid.*, 310.
- Lamb, H.: *Hydrodynamics*, Sixth Ed. (1945) Dover Publications, Inc., N. Y.
- Hill, S.: "Channelling in Packed Columns", *Chem. Eng. Sci. (1952) 1*, 247.
- Dietz, D. N.: "A Theoretical Approach to the Problem of Encroaching and By-Passing Edge Water", *Proc., Koninkl. Nederland, Akad. Wetenschap (1953) B 56*, 83.
- Van der Poel, C. and Killian, J. W.: "Attic Oil". Paper 919-G, presented at 32nd Annual Fall Meeting of Society of Petroleum Engineers in Dallas, Tex. (Oct. 6-9, 1957).
- Avsec, D.: *Publ. sci. et tech. ministere air (France) (1939) 155*, 21.
- Lewis, D. J.: *Proc. Roy. Soc. (London) (1950) A202*, 81.
- Van Meurs, P.: "The Use of Transparent Three-Dimensional Models for Studying the Mechanism of Flow Processes in Oil Reservoirs", *Trans. AIME (1957) 210*, 295.
- Van Meurs, P. and van der Poel, C.: "A Theoretical Description of Water-Drive Processes Involving Viscous Fingering", *Trans. AIME (1958) 213*, 103. ★★★